

Combinatorial Search for Green and Blue Phosphors of High Thermal Stabilities under UV Excitation Based on the $\text{K}(\text{Sr}_{1-x-y})\text{PO}_4:\text{Tb}^{3+}_x\text{Eu}^{2+}_y$ System

Ting-Shan Chan,^{†,‡} Yao-Min Liu,[†] and Ru-Shi Liu^{*,†}

Department of Chemistry, National Taiwan University, Taipei 106, Taiwan, and National Synchrotron Radiation Research Center, Hsinchu 300, Taiwan

Received April 16, 2008

The present investigation aims at the synthesis of $\text{KSr}_{1-x-y}\text{PO}_4:\text{Tb}^{3+}_x\text{Eu}^{2+}_y$ phosphors using the combinatorial chemistry method. We have developed square-type arrays consisting of 121 compositions to investigate the optimum composition and luminescence properties of KSrPO_4 host matrix under 365 nm ultraviolet (UV) light. The optimized compositions of phosphors were found to be $\text{KSr}_{0.93}\text{PO}_4:\text{Tb}^{3+}_{0.07}$ (green) and $\text{KSr}_{0.995}\text{PO}_4:\text{Eu}^{2+}_{0.005}$ (blue). These phosphors showed good thermal luminescence stability better than commercially available YAG:Ce at temperature above 200 °C. The result indicates that the $\text{KSr}_{1-x-y}\text{PO}_4:\text{Tb}^{3+}_x\text{Eu}^{2+}_y$ can be potentially useful as a UV radiation-converting phosphor for light-emitting diodes.

Introduction

Solid-state lighting, which uses light-emitting diodes (LEDs) for illumination, has attracted significant attention in recent years. Compared to conventional incandescent and fluorescent lamps, LED-based white light sources are superior in longer lifetime, higher energy efficiency, reliability, and environmentally friendly characteristics.^{1–3} The present strategy to produce white light uses combination of blue LED with yellow luminescence from YAG:Ce³⁺ phosphor materials.⁴ However, this strategy faces serious problems of poor color rendition, narrow visible range, and thermal quenching. As an alternative, a novel approach has been suggested that uses UV excitation to generate white LED. Therefore, it is necessary to develop novel red, green, or blue (RGB) phosphors, exhibiting high color purity and thermal stability in the UV-LEDs.⁵

On the other hand, the combinatorial chemistry was used to rapidly survey a wide range of compositions of phosphors under a variety of processing conditions.^{6–14} Moreover, some reviews on combinatorial methods materials science can be found in the previous reports.^{15–17} In this regard, our present combinatorial approach investigates the optimization of $\text{Y}_2\text{O}_3:\text{Bi}$, Eu red phosphors, which are excitable by 350–400 nm UV light, and study their energy-transfer effect.¹⁸ In this paper, we focus on the combinatorial search for green and blue phosphors excitable by UV radiation based on the $\text{K}(\text{Sr}_{1-x-y})\text{PO}_4:\text{Tb}^{3+}_x\text{Eu}^{2+}_y$ system. The optimum concentration was evaluated by screening of 121 compositions. The optimum concentration was reproduced by conventional bulk solid-state synthesis, and powder samples were analyzed in detail to obtain structure, photoluminescence and thermal

information. To the best of our knowledge, this is the first report to use combinatorial chemistry method assisted with solid state reaction to study Tb^{3+} and Eu^{2+} ions doped efficiently in a KSrPO_4 host.

Experimental Section

The detailed schematic diagram of the drop-on-demand inkjet delivery system can be found in a previous report.¹⁸ The eight independent piezoelectric inkjet heads and X–Y stage are controlled by the computer via the driving circuit and motor controller. Each inkjet head is connected to a suspension reservoir through a tube, and the substrate with a microreactor array is fixed on the stage. With the aid of a homemade inkjet delivery system, precursors (>99.99% purity) such as KH_2PO_4 , $\text{Sr}(\text{NO}_3)_2$, $\text{Eu}(\text{NO}_3)_3 \cdot 5\text{H}_2\text{O}$, and $\text{Tb}(\text{NO}_3)_3 \cdot 5\text{H}_2\text{O}$ were dissolved in deionizer water. Then the correct amount of each solution was collected in an Al_2O_3 ceramic substrate according to the composition map with the assistance of a computer-programmed inject system. The substrates containing the solutions were first dried at 100 °C for 1 h in an oven and then placed in a furnace where the temperature was slowly increased to 600 °C at the rate of 1 °C min^{-1} . Finally, the dried samples were pulverized and successively sintered at 1300 °C for 3 h under 5% H_2 /95% N_2 atmosphere. The emission spectra of the samples in the library were measured using an automatic system.¹⁹ The main parts of the system consist of an Hg Lamp, a portable optical fiber spectrometer (Ocean Optics, Inc., model SD2000), and an X–Y stage.

Two optimized compositions of $\text{KSr}_{0.93}\text{PO}_4:\text{Tb}^{3+}_{0.07}$ (green) and $\text{KSr}_{0.995}\text{PO}_4:\text{Eu}^{2+}_{0.005}$ (blue) phosphors were synthesized by conventional solid-state reaction using KH_2PO_4 , SrCO_3 , and Eu_2O_3 as raw materials. Stoichiometric homogeneous mixtures of highly pure raw materials were obtained by thorough grinding. The mixture was first calcined in air at

* To whom correspondence should be addressed. E-mail: rslu@ntu.edu.tw.

[†] Department of Chemistry.

[‡] National Synchrotron Radiation Research Center.

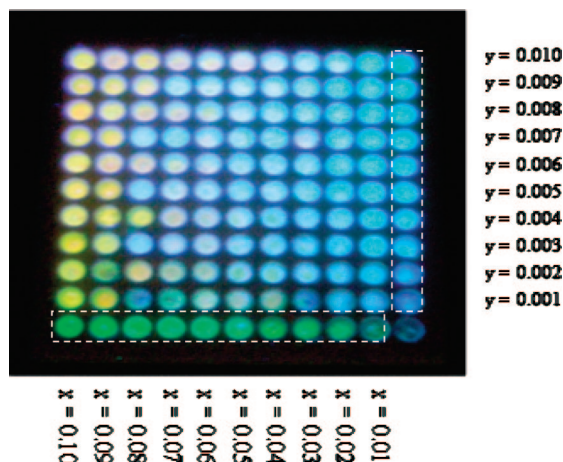


Figure 1. Composition map and photoluminescence photograph of the library excited under 365 nm UV light for $\text{KSr}_{1-x}\text{PO}_4:\text{Tb}^{3+}_x\text{Eu}^{2+}_y$.

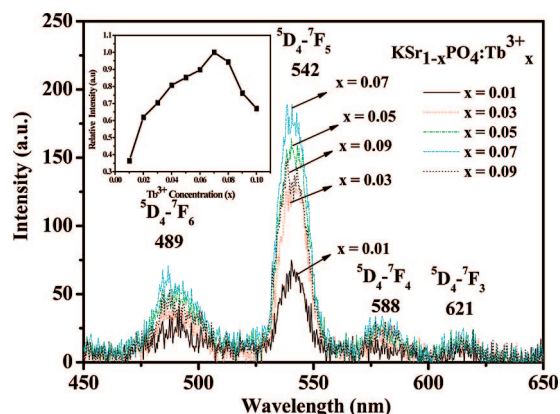


Figure 2. Emission spectra of $\text{KSr}_{1-x}\text{PO}_4:\text{Tb}^{3+}_x$ with different Tb^{3+} contents measured under 365 nm UV excitation. The normalized intensity as a function of Tb^{3+} concentration (x) is shown in the inset.

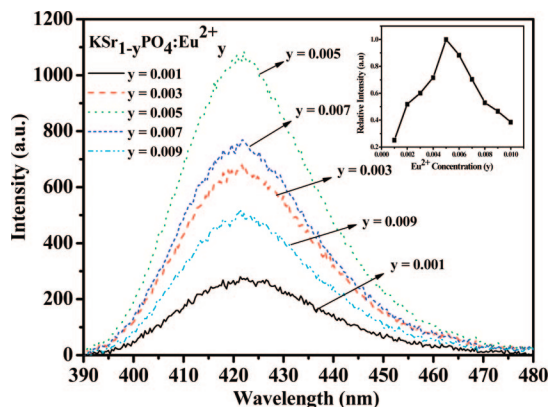


Figure 3. Emission spectrum of $\text{KSr}_{1-y}\text{PO}_4:\text{Eu}^{2+}_y$ with different Eu^{2+} contents measured under 365 nm UV excitation. The normalized intensity as a function of Eu^{2+} concentration (y) is shown in the inset.

600 °C for 3 h, followed by sintering in reductive atmosphere at 1300 °C for 3 h under 5% H_2 /95% N_2 atmosphere. The crystal structure and phase purity of the synthesized samples were identified by X-ray diffraction (XRD) analysis using X'Pert PRO advanced automatic diffractometer with $\text{Cu K}\alpha$ radiation operated at 45 kV and 40 mA. The GSAS program²⁰ was used for the Rietveld refinements to obtain the information on the crystal structures. The photolumines-

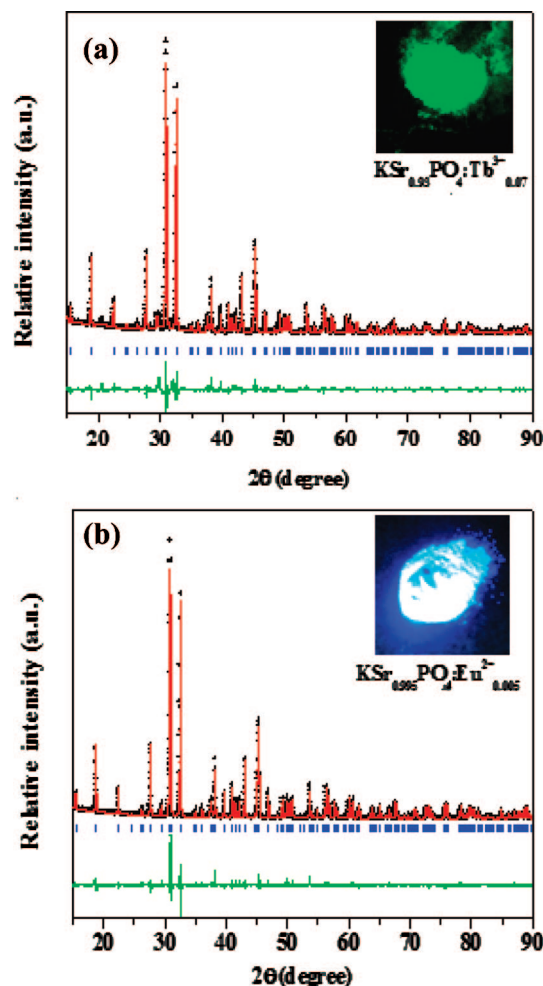


Figure 4. Observed (crosses), calculated (solid line), and differences (bottom) XRD Rietveld profiles of (a) $\text{KSr}_{0.93}\text{PO}_4:\text{Tb}^{3+}_{0.07}$ and (b) $\text{KSr}_{0.995}\text{PO}_4:\text{Eu}^{2+}_{0.005}$ at 300 K with $\lambda = 1.5406 \text{ \AA}$, respectively. Bragg reflections are indicated by tick marks.

cence (PL) of the samples were measured by using a FluoroMax-3 and FluoroMax-P. Thermal quenching measurements were investigated using a heating apparatus (THMS-600) in combination with the PL equipment.

Results and Discussion

The composition map and luminescent photograph of $\text{K}(\text{Sr}_{1-x-y})\text{PO}_4:\text{Tb}^{3+}_x\text{Eu}^{2+}_y$ library under 365 nm UV excitation are shown in Figure 1. The square-type arrays consist of 121 compositions with co-doped different Tb^{3+} contents from $x = 0.01$ to 0.1 and Eu^{2+} contents from $y = 0.001$ to 0.01. It is well-known that energy transfer is not possible between Tb^{3+} (4f–4f forbidden transition) and Eu^{2+} (5d–4f allowed transitions) because of the energy level. Hence, to clearly display the variation, in this paper we only focus on the high color purity green and blue phosphors (white area) by Tb^{3+} and Eu^{2+} doping, respectively, and ignore the effect of codoping.

Figure 2 presents the emission spectra of $\text{KSr}_{1-x}\text{PO}_4:\text{Tb}^{3+}_x$ ($x = 0.01, 0.03, 0.05, 0.07$ and 0.09), which varies with the Tb^{3+} contents in the library. The overall normalized intensity from $\lambda = 542 \text{ nm}$ according to Figure 2 is shown in the inset. The optimized composition of green phosphor was found to be $\text{KSr}_{0.93}\text{PO}_4:\text{Tb}^{3+}_{0.07}$. Under 365 nm UV light

Table 1. Crystallographic Data for $\text{KSr}_{0.93}\text{PO}_4:\text{Tb}^{3+}_{0.07}$ and $\text{KSr}_{0.995}\text{PO}_4:\text{Eu}^{2+}_{0.005}$ Phosphors

$\text{KSr}_{0.93}\text{PO}_4:\text{Tb}^{3+}_{0.07}$		$\text{KSr}_{0.995}\text{PO}_4:\text{Eu}^{2+}_{0.005}$	
space group	<i>Pnma</i> (orthorhombic)	Space group: <i>Pnma</i> (orthorhombic)	
cell parameter		Cell parameter	
<i>a</i>	7.3665 (1) Å	<i>a</i>	7.3679 (3) Å
<i>b</i>	5.5683 (1) Å	<i>b</i>	5.5661 (2) Å
<i>c</i>	9.6354 (2) Å	<i>c</i>	9.6431 (4) Å
$\alpha = \beta = \gamma$	90°	$\alpha = \beta = \gamma$	90°
cell volume	395.23(1) Å ³	cell volume	395.47(3) Å ³
reliability factors		reliability factors	
χ^2	1.5	χ^2	1.6
R_p	3.1%	R_p	3.1%
R_{wp}	4.8%	R_{wp}	4.9%

$\text{KSr}_{0.93}\text{PO}_4:\text{Tb}^{3+}_{0.07}$				
atoms	<i>x</i>	<i>y</i>	<i>z</i>	U_{iso} (Å ²)
K	0.15870	0.25000	0.58407	0.30
Sr	-0.00400	0.25000	0.19735	1.62
P	0.22613	0.25000	-0.08995	0.73
O(1)	0.30961	0.25000	0.05847	1.31
O(2)	0.29726	0.03013	0.84571	0.92
O(3)	0.52338	0.25000	0.58475	0.66
Tb	-0.00400	0.25000	0.19735	1.62

$\text{KSr}_{0.995}\text{PO}_4:\text{Eu}^{2+}_{0.005}$				
atoms	<i>x</i>	<i>y</i>	<i>z</i>	U_{iso} (Å ²)
K	0.16120	0.25000	0.58502	1.90
Sr	-0.00299	0.25000	0.19655	1.01
P	0.23382	0.25000	-0.07686	2.02
O(1)	0.31376	0.25000	0.06391	0.46
O(2)	0.28799	0.01393	0.85075	1.55
O(3)	0.52190	0.25000	0.59014	2.13
Eu	-0.00299	0.25000	0.19655	1.01

excitation, the major emission peak centering at 542 nm corresponds to $^5\text{D}_4-^7\text{F}_5$ transition, while $^5\text{D}_4-^7\text{F}_6$, $^5\text{D}_4-^7\text{F}_4$, and $^5\text{D}_4-^7\text{F}_3$ transition can be assigned to the emission peaks at 489, 588, 621 nm, respectively.

The emission spectra of $\text{KSr}_{1-y}\text{PO}_4:\text{Eu}^{2+}_y$ ($y = 0.001, 0.003, 0.005, 0.007, \text{ and } 0.009$) under 365 nm UV light excitation with different Eu^{2+} contents are shown in Figure 3. The overall normalized intensity from $\lambda = 424$ nm according to Figure 3 is also shown in the inset. The optimized composition of blue phosphor was found to be $\text{KSr}_{0.995}\text{PO}_4:\text{Eu}^{2+}_{0.005}$. The broad emission spectra with full

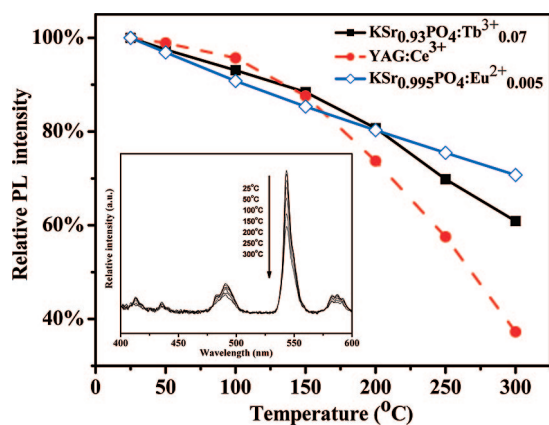


Figure 5. Temperature-dependent relative intensity of $\text{KSr}_{0.93}\text{PO}_4:\text{Tb}^{3+}_{0.07}$, $\text{KSr}_{0.995}\text{PO}_4:\text{Eu}^{2+}_{0.005}$, and commercially available YAG: Ce^{3+} phosphors. The select emission spectra as a function of temperature of $\text{KSr}_{0.93}\text{PO}_4:\text{Tb}^{3+}_{0.07}$ are shown in the inset.

width at half-maximum about 32 nm can be attributed to 5d–4f allowed transitions of Eu^{2+} ions.

Figure 4a and b shows observed (crossed), calculated (solid line), and difference (bottom) in XRD patterns of $\text{KSr}_{0.93}\text{PO}_4:\text{Tb}^{3+}_{0.07}$ and $\text{KSr}_{0.995}\text{PO}_4:\text{Eu}^{2+}_{0.005}$ phosphors at 300 K with $\lambda = 1.5406$ Å, respectively. Photographs for the $\text{KSr}_{0.93}\text{PO}_4:\text{Tb}^{3+}_{0.07}$ (green) and $\text{KSr}_{0.995}\text{PO}_4:\text{Eu}^{2+}_{0.005}$ (blue) phosphors under 365 nm UV light excitation are also shown in the inset. The observed peaks can be indexed on the basis of orthorhombic unit cell (space group *Pnma*), which is consistent with the JCPDS number-331045. The final structural parameters are given in Table 1. As noted from Table 1, Rietveld analysis afforded sufficiently low *R* factors for these two samples. Therefore, the optimization process by combinatorial chemistry method assisted with solid state reaction has been finely applied to novel phosphors development.

Figure 5 shows the temperature-dependent relative intensity of $\text{KSr}_{0.93}\text{PO}_4:\text{Tb}^{3+}_{0.07}$ (excitation at 365 nm and monitored at 542 nm), $\text{KSr}_{0.995}\text{PO}_4:\text{Eu}^{2+}_{0.005}$ (excitation at 365 nm and monitored at 424 nm), and commercially YAG: Ce^{3+} (excitation at 460 nm and monitored at 550 nm) phosphors. The selected emission spectra as a function of temperature of $\text{KSr}_{0.93}\text{PO}_4:\text{Tb}^{3+}_{0.07}$ are also shown in the inset. As seen from Figure 5, the relative peak intensity decreases from initial 100% at 30 °C to ~62% ($\text{KSr}_{0.93}\text{PO}_4:\text{Tb}^{3+}_{0.07}$), ~72% ($\text{KSr}_{0.995}\text{PO}_4:\text{Eu}^{2+}_{0.005}$), and ~38% (YAG: Ce^{3+}) at 300 °C, respectively. The result indicated that the thermal luminescence stability of $\text{KSr}_{0.93}\text{PO}_4:\text{Tb}^{3+}_{0.07}$ (green) and $\text{KSr}_{0.995}\text{PO}_4:\text{Eu}^{2+}_{0.005}$ (blue) phosphors above 200 °C was higher than the commercially available YAG: Ce^{3+} .

Conclusion

We have synthesized green and blue phosphate phosphors for $\text{K}(\text{Sr}_{1-x-y})\text{PO}_4:\text{Tb}^{3+}_x\text{Eu}^{2+}_y$ by using the combinatorial chemistry method. The two optimum compositions were found to be $\text{KSr}_{0.93}\text{PO}_4:\text{Tb}^{3+}_{0.07}$ (green) and $\text{KSr}_{0.995}\text{PO}_4:\text{Eu}^{2+}_{0.005}$ (blue). To confirm the composition and characterization of the structure and thermal luminescence properties in detail, the samples were synthesized through solid-state reaction under the same condition. We demonstrate that the thermal stabilities of $\text{K}(\text{Sr}_{1-x-y})\text{PO}_4:\text{Tb}^{3+}_x\text{Eu}^{2+}_y$ are higher than the commercially YAG: Ce^{3+} . On the basis of the above results, it is reasonable to believe that the developed combinatorial chemistry method makes the search for high efficiency phosphors for use in UV-LEDs possible.

Acknowledgment. We thank the National Science Council of Taiwan (Grant NSC 96-2120-M-002-019) and the Ministry of Economic Affairs of Taiwan. (Grant 96-EC-17-A-07-S1-043) for financial supports.

References and Notes

- (1) Neeraj, S.; Kijima, N.; Cheetham, A. K. *Chem. Phys. Lett.* **2004**, *387*, 2.
- (2) Nishida, T.; Ban, T.; Kobayashi, N. *Appl. Phys. Lett.* **2003**, *82*, 3817.
- (3) Kim, J. S.; Jeon, P. E.; Choi, J. C.; Park, H. L.; Mho, S. I.; Kim, G. C. *Appl. Phys. Lett.* **2004**, *84*, 2931.
- (4) Nakamura, S.; Fasol, G. *The Blue Laser Diode: GaN Based Light Emitters Lasers*; Springer: Berlin, 1997.

- (5) Shimizu, Y.; Sakano, K.; Noguchi, Y.; Moriguchi, T. U.S. Patent 5,998,925, 1999.
- (6) Sun, X. D.; Gao, C.; Wang, J.; Xiang, X.-D. *Appl. Phys. Lett.* **2007**, *70*, 3353.
- (7) Wang, J.; Yoo, Y.; Gao, C.; Takeuchi, I.; Sun, X.; Chang, H.; Xinag, X.-D.; Schultz, P. G. *Science* **1998**, *279*, 1712.
- (8) Sohn, K. S.; Park, E. S.; Kim, C. H.; Park, H. D. *J. Electrochem. Soc.* **2000**, *147*, 4368.
- (9) Sohn, K. S.; Seo, S. Y.; Park, H. D. *Electrochem. Solid-State Lett.* **2001**, *4*, H26.
- (10) Sohn, K. S.; Kim, C. H.; Park, J. T.; Park, H. D. *J. Mater. Res.* **2002**, *17*, 3201.
- (11) Seo, S. Y.; Sohn, K. S.; Park, H. D.; Lee, S. *J. Electrochem. Soc.* **2002**, *149*, H12.
- (12) Chen, L.; Bao, J.; Gao, C. *J. Comb. Chem.* **2004**, *6*, 699.
- (13) Luo, Z. L.; Geng, B.; Bao, J.; Gao, C. *J. Comb. Chem.* **2005**, *7*, 942.
- (14) Sohn, K. S.; Park, D. H.; Cho, S. H.; Kim, B. I.; Woo, S. I. *J. Comb. Chem.* **2006**, *8*, 44.
- (15) Jandeleit, B.; Schaefer, D. J.; Powers, T. S.; Turner, H. W.; Weinberg, W. H. *Angew. Chem., Int. Ed.* **1999**, *38*, 2494.
- (16) Michael, A. R. M. R. H.; Ulrich, S. S. *Macromol. Rapid Commun.* **2003**, *24*, 16.
- (17) Stefan, S.; Michael, A. R. M.; Ulrich, S. S. *Macromol. Rapid Commun.* **2004**, *25*, 21.
- (18) Chan, T. S.; Kang, C. C.; Liu, R. S.; Chen, L.; Liu, X. N.; Ding, J. J.; Bao, J.; Gao, C. *J. Comb. Chem.* **2007**, *9*, 343.
- (19) Chen, L.; Bao, J.; Gao, C. *J. Comb. Chem.* **2004**, *6*, 699.
- (20) Larson, A. C.; Von Dreele, R. B. *Generalized Structure Analysis System (GSAS)*; Report LAUR 86-748; Los Alamos National Laboratory: Los Alamos, NM, 1994.

CC800060X